JOURNAL OF GEOPHYSICAL RESEARCH, VOL. ???, XXXX, DOI:10.1029/,

Dominant aerosol processes during high-pollution episodes over Greater Tokyo

K.N. Sartelet

CEREA, Research Center for Atmospheric Environment, Joint Laboratory Ecole Nationale des Ponts et Chaussées and Electricité de France, France

H. Hayami

Central Research Institute of Electric Power Industry, Abiko, Chiba, Japan

B. Sportisse

CEREA, Research Center for Atmospheric Environment, Joint Laboratory Ecole Nationale des Ponts et Chaussées and Electricité de France, France

Abstract.

This paper studies two high-pollution episodes over Greater Tokyo: 9 and 10 December 1999, and 31 July and 1 August 2001. Results obtained with the chemistry-transport model (CTM) Polair3D are compared to measurements of inorganic $PM_{2.5}$. To understand to which extent the aerosol processes modeled in Polair3D impact simulated inorganic $PM_{2.5}$, Polair3D is run with different options in the aerosol module, e.g. with/without heterogeneous reactions. To quantify the impact of processes outside the aerosol module, simulations are also done with another CTM (CMAQ).

In the winter episode, sulfate is mostly impacted by condensation, coagulation, long-range transport, and deposition to a lesser extent. In the summer episode, the effect of long-range transport largely dominates. The impact of condensation/evaporation is dominant for ammonium, nitrate and chloride in both episodes. However, the impact of the thermodynamic equilibrium assumption is limited. The impact of heterogeneous reactions is large for nitrate and ammonium, and taking heterogeneous reactions into account appears to be crucial in predicting the peaks of nitrate and ammonium. The impact of deposition is the same for all inorganic $PM_{2.5}$. It is small compared to the impact of other processes although it is not negligible. The impact of nucleation is negligible in the summer episode, and small in the winter episode. The impact of coagulation is larger in the winter episode than in the summer episode, because the number of small particles is higher in the winter episode as a consequence of nucleation.

1. Introduction

With the impact of air pollution on health and vegetation being a great concern, chemical transport models (CTMs) are often used at a regional scale to predict air quality, i.e. to compute the distribution of atmospheric gases, aqueous phase species and particulate matter. High pollution episodes may occur depending on emissions and sources of pollutants, as well as on the dynamical characteristics of the meteorology.

The meteorology over Greater Tokyo is strongly influenced by orography and sea/land breeze regimes, as shown by *Fujibe* [1985] and *Ohara et al.* [1990]. High pollution episodes are often observed in early summer and early winter. Early winter episodes are often a consequence of the meso-synoptic scale meteorology (*Mizuno and Kondo* [1992], *Uno et al.* [1996], *Ohara et al.* [2003]): sea/land breeze and the blocking effect of orography in central Japan. These episodes are characterized by high NO_2 and chloride concentrations (*Uno et al.* [1996], *Kaneyasu et al.* [1989]). Measurements made by *Kaneyasu et al.* [1989] suggest that the precursor HNO_3 of aerosol nitrate is formed by photochemical reactions,

0148-0227/08/$9.00

while the precursor of aerosol chloride may be locally emitted. For summer episodes, the role of sea breeze penetration for oxidants is detailed by *Wakamatsu et al.* [1999]. *Hayami* [2003] founds that the PM mass completely changes in proportion to RH in an episode that happened within 24 hours. Rapidly increasing RH may enhance condensation onto aerosols.

Two episodes are studied in this paper: one early winter episode (9 and 10 December 1999), and one summer episode (31 July and 1 August 2001). These episodes are simulated using the CTM Polair3D (*Boutahar et al.* [2004]). This paper aims at studying the impact of different aerosol processes that may influence the particle concentrations observed during these episodes. Furthermore, the impact of the aerosol processes is compared to the impact of numerical choices made in the aerosol model. For example, the impact of the size distribution is studied by replacing the modal aerosol model MAM (*Sartelet et al.* [2006]) used in Polair3D by a sectional model (SIREAM: *Debry et al.* [2007]). Aerosol concentrations are not only influenced by the aerosol model, but also by the parameterizations and the numerical schemes used for advection, diffusion, chemical mechanism (*Mallet and Sportisse* [2006]). To have an estimate of how these processes may influence the concentrations, the impact of the different aerosol processes is compared to the impact of using a different CTM (CMAQ, *Binkowski and Roselle* [2003], *Eder and Yu* [2006], *Yu et al.* [2006b], *Eder et al.* [2006]).

2. The Models

The CTM Polair3D (*Boutahar et al.* [2004]) is used with the chemical mechanism RACM (*Stockwell et al.* [1997]). Photolysis rates are computed off-line, as done in the photolysis rate preprocessor of CMAQ (*Roselle et al.* [1999]). Vertical diffusion is computed using the Troen and Mahrt's parameterization (*Troen and Mahrt* [1986]) within the boundary layer, and using the Louis' parameterization (*Louis* [1979]) above it. Polair3D may be used with two aerosol models : MAM (*Sartelet et al.* [2006]) and SIREAM (*Debry et al.* [2007]). The difference between the models lies in the size distribution: in MAM the size distribution is modeled with four log-normal modes (modes i, j, k, c), and in SIREAM it is modeled with sections. Four sections are used in the simulations of this paper. In MAM and SIREAM, the modes/sections are bounded as follow: mode i: $< 0.01\mu$m, mode j: [0.01; 0.1μm], mode k: [0.1; 2.5μm], mode c: $> 2.5\mu$m. A complete technical description of MAM and SIREAM may be found in *Sportisse et al.* [2006]. MAM is used for the simulations of this paper, except when specified. It is now briefly described.

2.1. Composition

Particles can be made of inert species (dust and elemental carbon), liquid water, inorganic species (sodium, chloride, ammonium, nitrate and sulfate) and organic species.

2.2. Aerosol Processes

Coagulation, condensation/evaporation and nucleation are modeled as described in *Sartelet et al.* [2006].

2.2.1. Condensation/evaporation

Condensation/evaporation is computed using the thermodynamic module ISORROPIA (*Nenes et al.* [1998]). By default, thermodynamic equilibrium is assumed between the gas and the aerosol phases. However, Po-

lair3D may also be used without the assumption of thermodynamic equilibrium for large modes/bins, for which condensation/evaporation is then computed dynamically. Although the thermodynamic equilibrium assumption may not be valid especially for large aerosols, it is used in the baseline simulations here because it is computationally efficient. The effect of this assumption is studied in a separate sensitivity simulation

2.2.2. Nucleation

Nucleation is modeled using the ternary parameterization (water, ammonium and sulfate) of Napari (*Napari et al.* [2002]). The ternary nucleation rate is several order of magnitudes larger than commonly used binary nucleation rates (water and sulfate).

2.2.3. Heterogeneous reactions

In the first runs presented here, heterogeneous reactions are not taken into account in Polair3D. If heterogeneous reactions are taken into account in Polair3D, they are modeled according to *Jacob* [2000]: $HO_2 \rightarrow 0.5\ H_2O_2$, $NO_2 \rightarrow 0.5\ HONO + HNO_3$, $NO_3 \rightarrow HNO_3$, $N_2O_5 \rightarrow 2\ HNO_3$. The kinetic rates of these first order reactions are $k_i = \left(\frac{a}{D_i^g} + \frac{4}{\bar{c}_i^g \gamma}\right)^{-1} S_a$, where a is the particle radius, $\bar{c}_i^g$ is the gas-phase thermal velocity in the air, S_a is the available surface of condensed matter per air volume, and γ is the reaction probability that a molecule impacting the aerosol surface undergoes reaction. γ strongly depends on the chemical and size distribution of particles. The values used in this paper are $\gamma_{HO_2} = 0.2$, $\gamma_{NO_2} = 10^{-4}$, $\gamma_{NO_3} = 10^{-3}$ and $\gamma_{N_2O_5} = 0.03$.

2.2.4. Dry deposition

Dry deposition is parameterized with a resistance approach following *Zhang et al.* [2001]. The processes modeled include gravitational settling and the deposition processes of Brownian diffusion, impaction, interception, particle rebound. The aerodynamic resistance and the friction velocity are computed as in CMAQ (*Binkowski and Roselle* [2003]). Dry deposition depends on the diameter of the particles. In Polair3D-MAM, for each lognormal mode and each moment, the deposition velocity is integrated over diameters by fourth order Gauss-Hermite quadratures. In Polair3D-SIREAM, the mean diameter of each section is used to compute the deposition velocities.

2.2.5. Mode Merging versus Mode splitting

A mode merging scheme or a mode splitting scheme is required in a modal model to prevent modes from overlapping, i.e. to force modes to be of distinct size ranges throughout the simulations. Different mode merging schemes may be used, often based on that of *Binkowski and Roselle* [2003], where the threshold diameter between the two modes to be merged is chosen as the diameter where the number distributions of the two modes overlap. In Polair3D, mode merging is applied between modes i and j (and between modes j and k), when the diameter of the volume distribution of mode i (and mode k) exceeds a fixed diameter of $0.01\mu m$ for mode i (and of $0.1\mu m$ for mode j).

In the tests performed later in this paper, the mode merging scheme is replaced by a mode splitting scheme (*Sartelet et al.* [2006]), which is designed to reproduce the evaluation of a mode that splits into two modes under the combined effect of nucleation, condensation and coagulation.

For the simulations done with CMAQ (*Binkowski and Roselle* [2003], *Mebust et al.* [2003], *CMAQ* [1999]), the version 4.3 is used, with the Carbon Bond IV chemical mechanism (*Gery et al.* [1989]). It is modified to include sodium and chloride in the Aitken and in the ac-

cumulation modes. In CMAQ, the aerosol module is a modal one with 3 modes. As in Polair3D, the following processes are taken into account: coagulation, condensation/evaporation, nucleation, heterogeneous reactions, dry deposition. For condensation/evaporation, thermodynamic equilibrium is assumed between the gas and the aerosol phases. Nucleation is modeled with a binary nucleation rate. The heterogeneous reaction $N_2O_5 \rightarrow 2\ HNO_3$ is taken into account.

3. Domain and Input Data

Simulations are performed over a 210km x 240km area, centered around Tokyo, with a 5km x 5km resolution (Figure 1 shows the domain of simulation, which is discretized with 42 x 48 points). The horizontal domain is the same for the simulations done with Polair3D and CMAQ. For simulations with Polair3D, 12 vertical layers are considered (0m, 29m, 58m, 103m, 147m, 296m, 447m, 677m, 954m, 1282m, 1705m, 2193m, 2761m). A no-flux boundary condition (free atmosphere) is used at the top boundary for diffusion. In CMAQ, 16 layers of varying thickness extend to about 16km height. The vertical coordinate is not altitude but sigma-levels. The averaged altitudes of the first 10 layers of CMAQ correspond to the altitudes used in Polair3D. Meteorological data are provided by the Japanese Meteorological Agency with a 20km x 20km resolution every six hours. Finer hourly meteorological data, with a 5km x 5km resolution are obtained by running the meteorological model MM5, the Fifth-Generation Pennsylvania State University/National Center for Atmospheric Research (NCAR) Mesoscale model (*Grell et al.* [1994]). Initial and boundary conditions (with inputs varying every three hours) are obtained by running the CTM CMAQ over East Asia with a 45km x 45km resolution. Emission inventories are provided by a collaboration with the Japanese National Institute for Environmental Studies (*Hayami and Kobayashi* [2004]). Emission sources include mobile sources (road, air, vessels), stationary sources (domestic, industries), waste water treatment, biogenic/natural sources (agriculture, soil, volcanoes). Table 1 summarizes the total amount of emitted particulate matter and precursors over the domain. The emission inventory does not contain information about either the size distribution or the chemical speciation. The size distribution and the chemical speciation of PM_{10} and $PM_{2.5}$ are specified as in CMAQ (*Binkowski and Roselle* [2003]). All $PM_{10} - PM_{2.5}$ are assigned to the coarse mode and particles are assumed to be made of 90% dust and 10% elementary carbon. Most of $PM_{2.5}$ (99.9%) are assigned to the accumulation mode, and 0.1% to the Aitken mode. For $PM_{2.5}$, particles are assumed to be made of 30% dust and 70% elementary carbon. The parameters of the three modes used for emission are shown in Table 2. Whereas the modal model in CMAQ has three modes (aitken, accumulation and coarse), the modal model in MAM has an additional mode designed for nanometer nucleated particles. This mode is not used for emission.

For gaseous species, dry deposition velocities are computed off-line following *Wesely* [1989].

Simulations start one day before the episode to allow for spin-up. Tests using two days for spin-up showed that one day spin-up is sufficient for the gaseous and $PM_{2.5}$ concentrations considered here.

4. Description of The Episodes

4.1. 9^{th} and 10^{th} December 1999

During this episode, chemical concentrations are observed to be high. On the 9^{th}, this is mostly due, to the presence of a meso-front. Strong cold winds coming from West and North West stay weak at low altitudes because of the presence of orography in the West and in the North West. Warm winds from South do not penetrate much in land and a meso-front is observed (black dashed line in Figure 2). As shown in Figure 2, the meso-front is not so well reproduced by MM5. On the 9^{th}, pollutants accumulate in the Northern part of the front. This is seen in Figure 3, which shows high nitrate concentrations in the Northern part of the front at 6pm. Sulfate concentrations are also high where ammonium and nitrate concentrations are high, but sulfate concentrations are even higher over sea. These high concentrations are brought from South West, but they do not propagate much over land because of the meso front. On the 10^{th}, high concentrations are a consequence of weak winds and high pollution.

4.2. 31^{st} July and 1^{st} August 2001

The episode of 31 July and 1 August 2001 is characteristic of sea and land breeze circulation. Wind patterns are also influenced by local winds.

On 31 July, winds are weak over the whole domain. Winds from west and south west strengthen during the day, and penetrate on land as the temperature on land gets warmer than the temperature on sea. Figure 4 displays the wind vector at 2pm on 31 July. High sulfate concentrations are brought from the south west. At 2pm, sulfate concentrations are high over almost the whole domain, as can be seen in Figure 5.

On 31 July at night, although south westerly winds are strong over sea, winds stay low on land. In the early morning of 1 August, south westerly winds weaken. They do not penetrate much on land, and winds on land stay low.

5. Comparison to Measurements

5.1. Measurements

Aerosol distributions were collected using impactor, denuder, and filter pack (*Hayami and Fujita* [2004]), every three hours, except for the summer 2001 where at night they were collected every six hours. Hourly gaseous distributions at different stations distributed over Greater Tokyo are provided by Japanese local institute governments.

The stations at which comparisons are made are shown in Figure 1.

On 9 and 10 December 1999, for gas, data are available for O_3, NO_x and SO_2 at 3 sites: Yokosuka, Fukaya and Kudan. For $PM_{2.5}$, data are available for sulfate, ammonium, nitrate and chloride at 4 sites: Yokosuka, Omiya, Fukaya and Kudan (Tokyo).

On 31 July and 1 August 2001, data are available at two sites: Kumagaya and Komae, for O_3, NO_x, SO_2 and $PM_{2.5}$.

Sulfate concentrations are overall higher on 31 July and 1 August 2001 than on 9 and 10 December 1999, with an average over the stations of 13.3μg m^{-3} against 2.6μg m^{-3}. Furthermore, sulfate represents as much as 50% of the inorganic $PM_{2.5}$ in the summer episode, against 21% in the winter one. Ammonium and nitrate concentrations are also higher on 31 July and 1 August

2001 than on 9 and 10 December 1999, with an average of 7.7μg m^{-3} against 2.7μg m^{-3} for ammonium, and 5.7μg m^{-3} against 4.5μg m^{-3} for nitrate.

5.2. Statistics

Comparison of the results obtained with Polair3D to measurements is done for inorganic fine aerosols ($PM_{2.5}$). Model results for this comparison take into account data only from the grid boxes for which observations are available. In MAM/SIREAM, $PM_{2.5}$ are computed by summing the three smallest modes/sections (modes i, j and k). Similarly, in CMAQ, as the mode i is not modeled, the two smallest modes, i.e. j and k, are summed up to compute $PM_{2.5}$

The relative bias and error between modeled and observed concentrations are quantified using unbiased symmetric metrics (*Yu et al.* [2006]): the normalized mean bias factor B_{NMBF} and the normalized mean absolute error factor E_{NMAEF} (Appendix A). The correlation coefficient (%) is also used as a statistical indicator. The smaller the bias and the error are, and the larger the correlation is, the closer the model fits the observation. Bias indicates whether the model tends to under or overpredict the observation, and error indicates how large the deviation is.

Yu et al. [2006] suggests the criteria of model performance for sulfate to be taken as $|B_{NMBF}| \leq 25\%$ and $E_{NMAEF} \leq 35\%$.

5.3. 9^{th} and 10^{th} December 1999

The statistical indicators are shown in Table 3. The model satisfies the criteria suggested by *Yu et al.* [2006] for sulfate. However, these criteria are not satisfied for ammonium, nitrate and chloride, which are more difficult to model because of their volatility. This difficulty to model nitrate and ammonium is stressed for example by *Zhang et al.* [2006] where nitrate and ammonium are underpredicted by factors 9.6 and 2.1 respectively in the Southeastern US for the period of 1-10 July 1999.

The correlation coefficients are good for all species, ranging from 66% for sulfate to 36% for chloride. This suggests that the overall diurnal patterns are well modeled. As shown in Figure 8, the majority of hourly simulations falls within a factor 2 of the observations for sulfate and for high values of nitrate and ammonium. However, values lower than about 3μg m^{-3} for ammonium and 5μg m^{-3} for nitrate are often scattered outside the factor of two reference line.

The presence of the meso-front in the afternoon of 9 December may be seen from the concentrations of $PM_{2.5}$ in Figures 6 and 7. Nitrate and ammonium concentrations are high in the afternoon before 6pm at Omiya and Fukaya, which are located in the northern part of the front where the pollutants accumulate. However, they are low at Yokosuka, which is located in the south part of the front. Kudan is located close to the front at 6pm. Concentrations are low at Kudan before 6pm and the concentrations of pollutants increase at Kudan from 6pm. On 10 December, pollutants are observed to be high at the four stations, as a consequence of weak winds.

Polair3D tends to over-estimate sulfate as shown by the B_{NMBF}, which is as high as 0.26. As shown in Figures 6 and 7, sulfate is overestimated in the evening of the 10^{th}. For both ammonium and nitrate, although the position of the peaks in time is well predicted by Polair3D, they are under-estimated at Fukaya and Omiya on the 9^{th}. To find the reason of the discrepancies between simulations and measurements on the 9^{th} for the peaks of nitrate and ammonium at Fukaya and Omiya,

the sensitivity of the amplitude of these peaks to options in the aerosol module is studied in the next section. Ammonium is overall over-estimated, while nitrate and chloride are under-estimated. However, for both nitrate and ammonium, the model has difficulties to predict the low concentrations in the night between the 9^{th} and the 10^{th} at Omiya and Fukaya, as confirmed by the scatter plots. The reason for this discrepancy is also investigated in the next section.

5.4. 31^{st} July and 1^{st} August 2001

Comparisons of the results obtained with Polair3D are shown in Figure 9 for $PM_{2.5}$.

The statistical indicators are shown in Table 4 for 31 July and 1 August 2001. As for 9 and 10 December 1999, the model satisfies the criteria suggested by *Yu et al.* [2006] for sulfate. However, these criteria are again not satisfied for ammonium and nitrate. Because chloride concentrations are very low in this summer run, they are not shown.

As for the winter episode, the majority of hourly simulations falls within a factor 2 of the observations for sulfate (Figure 8). The majority of hourly simulation falls within a factor 2 of the observation at Komae, but scatter outside the reference lines is observed at Kumagaya. Considerable scatter is observed for nitrate at both Komae and Kumagaya with many simulated values falling outside the factor of two reference lines.

The correlation coefficient is low for sulfate (-2%). For example, the model predicts a decrease in sulfate concentrations in the morning of 31 July at both Komae and Kumagaya (Figure 9), which is not confirmed by observations. Because this episode is a clear-sky one, cloud chemistry does not influence sulfate concentrations. Sulfate may be produced by the condensation of H_2SO_4, or it may be transported to the domain of study through boundary conditions. H_2SO_4 is either directly emitted or produced by the reaction of SO_2 with OH. However, although the correlation coefficient is low for sulfate, good correlation is observed for SO_2 (Table 4). This suggests that uncertainty in sulfate concentrations is linked to uncertainty in the H_2SO_4 emissions and in the sulfate boundary conditions.

The sulfate concentrations, which are quite high all through the episode, are relatively well modeled. However, the measured concentrations do not vary much, whereas the model exhibits stronger time variations. For ammonium, although results are close to measurements at Komae, ammonium is under-estimated at Kumagaya. According to measurements, ammonium concentrations are twice as high in Kumagaya as in Komae. These high concentrations in Kumagaya are not reproduced by the models. Nitrate is severely under-estimated at both Kumagaya and Komae. The reasons for the discrepancies between measurements and modeled concentrations are investigated in the next section.

6. Impact of Aerosol Processes

The impact of different processes on aerosol concentrations is investigated for both episodes. The following processes are considered: nucleation, coagulation, condensation/evaporation, dry deposition, heterogeneous reactions. The impact of numerical schemes in the aerosol module is also studied: size-distribution and mode merging/splitting.

The impact of each of these physical and numerical processes is quantified by comparing a simulation S_p

where only a process p is ignored (or its parameterization is changed) to the reference simulation S_r where all the processes are taken into account. The simulations S_p are successively: a simulation without condensation/evaporation, a hybrid simulation (thermodynamic equilibrium is only assumed for the smallest mode instead of being assumed for the four modes), a simulation with heterogeneous reactions (heterogeneous reactions are not taken into account in the reference simulation S_r), a simulation with only the N_2O_5 heterogeneous reaction, a simulation without the NO_2 heterogeneous reaction, a simulation without deposition, a simulation without nucleation, a simulation without coagulation, a simulation done using SIREAM instead of MAM (the log-normal size distribution is replaced by a sectional distribution), a simulation done using mode splitting instead of mode merging, and a simulation without neither mode splitting nor mode merging. The quantification of the impact of each process p is done by computing the B_{NMBF} and the E_{NMAEF} between S_p and S_r at the sites where measurements are made. The larger in absolute value the B_{NMBF} and the E_{NMAEF} are, the stronger the impact of the process p is. The statistics B_{NMBF} and E_{NMAEF} between CMAQ and S_r are also computed in order to compare the impact of using a different chemistry transport model to the impact of each of the processes p. CMAQ takes into account condensation/evaporation with the same thermodynamic model as Polair3D (Isorropia), the heterogeneous reaction of N_2O_5, deposition, nucleation and mode merging. The comparisons of simulations done with Polair3D allow us to quantify the uncertainty related to the aerosol module. By using CMAQ, the simulated $PM_{2.5}$ concentrations may vary not only because of uncertainty in the aerosol module, but also because of uncertainties in chemistry, transport and diffusion. For example, even though Polair3D and CMAQ use the same meteorological fields, uncertainties in transport may be linked to the numerical schemes used, uncertainty in diffusion is related to the modeling of vertical diffusion.

Because the reference run does not always capture the observed behavior or because it may capture it for wrong reasons (e.g. inaccuracies in several processes cancel each other out), changing processes one at a time does not automatically give a reliable estimate of the relative importance of these processes in the real world, but only in the model. Similarily, the comparison of two CTMs does only give an estimate of the uncertainty related to transport, chemistry and diffusion, as these could be described inaccurately in both models.

Tables 5 and 6 compare the reference simulation S_r to different simulations S_p for 9 and 10 December 1999 and 31 July and 1 August 2001 respectively. For both episodes, the impact of heterogeneous reactions is large for nitrate and ammonium (the E_{NMAEF}s are as large as 1.95 and 0.79 respectively in winter). The HNO_3 produced by heterogeneous reactions condenses onto aerosols to form nitrate, and the available ammonia condenses to neutralize the nitrate. Concentrations of nitrate and ammonium increase by taking into account heterogeneous reactions, as shown by the positive B_{NMBF}. The impact of heterogeneous reactions on sulfate is small. The H_2O_2 concentration produced by heterogeneous reactions does not influence sulfate concentrations because aqueous chemistry is not taken into account. The impact of condensation/evaporation is preponderant for ammonium, nitrate and chloride (for nitrate, the E_{NMAEF} is as large as 2.44 in the winter episode and 96.4 in the summer episode). This impact is even larger than the impact of using CMAQ, or the impact of heterogeneous

reactions. Condensation is largely preponderant over evaporation as seen by the negative B_{NMBF}. Because of the low-volatility of sulfate, the impact of the hybrid scheme is small for sulfate (with a E_{NMAEF} under 0.07). It is larger for other inorganic species, such as ammonium and nitrate, which are influenced by whether condensation/evaporation is computed dynamically or by assuming thermodynamic equilibrium. The hybrid scheme mostly influences ammonium in the winter case with a E_{NMAEF} of 0.41, and it influences mostly nitrate in the summer case with a E_{NMAEF} of 0.49. Because coagulation and deposition do not differentiate the chemical composition of aerosols, their impacts are the same for each chemical species. The impact of deposition is between 0.08 and 0.10 for each species for both the winter and the summer simulations. Not taking deposition into account, leads as expected to an increase in aerosol concentrations as shown by the positive B_{NMBF}. The impact of nucleation is small, with E_{NMAEF} smaller than 0.06. Although a large number of nanometer particles are created by nucleation (the ternary nucleation scheme is several order of magnitudes larger than commonly used binary nucleation schemes), the mass produced is small compared to the mass of $PM_{2.5}$. Furthermore, although the nucleated particles are made of sulfate and ammonium, nitrate and chloride are also influenced by nucleation, as they may condense onto freshly nucleated particles. Considering numerical processes, the impact of mode splitting and mode merging is negligible with E_{NMAEF} smaller than 0.03. Mode merging/splitting influence the smaller particles, which do not contribute much to the mass of $PM_{2.5}$. The impact of using SIREAM, although not negligible, is not large for sulfate with E_{NMAEF} under 0.09. The impact is larger for nitrate, especially in the summer episode, where the E_{NMAEF} reaches 0.22. A small impact on sulfate concentrations may correspond to larger impacts on other inorganic semi-volatile components. During condensation/evaporation, ammonium, nitrate and chloride are not only influenced by the size distribution of aerosols, but also by the internal composition because of their volatility.

6.1. 9^{th} and 10^{th} December 1999

In the winter episode of 1999, for sulfate, there is a dominant impact of both condensation and coagulation with E_{NMAEF} as large as 0.27 and 0.21 respectively. These impacts are of the same order of magnitude as those of CMAQ (the E_{NMAEF} is 0.23). For sulfate, the impacts of other processes are small, except for deposition, for which E_{NMAEF} is equal to 0.10. Sulfate is produced by the condensation of H_2SO_4 and by the transport from outside the model domain through boundary conditions. Because sulfate decreases only by a factor 1.27 if condensation is not taken into account, the impact of long-range transport is likely to be high. The boundary condition for sulfate averaged over time, latitude and longitude is 3.0 μg m^{-3}, against a mean concentration of 3.5 μg m^{-3} in the domain of study. For other species, the impact of condensation/evaporation largely dominates, with E_{NMAEF} as large as 3.92 for chloride, 2.44 for nitrate and 1.04 for ammonium. This indicates that chloride, nitrate and ammonium are strongly influenced by local conditions. The impact of heterogeneous reactions is important for nitrate and ammonium with a E_{NMAEF} as large as 1.95 and 0.79. The dominant heterogeneous reactions are the N_2O_5 and the NO_2 heterogeneous reactions. The E_{NMAEF} is as high as 0.94 and 0.38 for nitrate and ammonium when only the N_2O_5 heterogeneous reaction is taken into account. A simulation without the NO_2

heterogeneous reaction but with all the other three gives similar results to the simulation with only the N_2O_5 heterogeneous reaction. The impact of the hybrid scheme is important for ammonium with a E_{NMAEF} of 0.41, which is as large as the impact of using CMAQ (0.38). However, the impact is smaller for other chemical species, with a E_{NMAEF} of 0.13 for nitrate against a E_{NMAEF} of 1.0 when CMAQ is used. Coagulation has an impact almost as large as the impact of condensation or the impact of CMAQ for sulfate with a E_{NMAEF} of 0.21. Although the impact of coagulation is the same for each chemical species, it is less important for nitrate, ammonium and chloride in comparison to the impact of other processes. Although nucleation is small, it is not negligible with a E_{NMAEF} of 0.05 for sulfate and ammonium.

The impacts of the dominant processes during the episode are now investigated in more details, aiming at understanding the potential reasons for the discrepancies between measurements and simulated concentrations at the different stations (Figures 6 and 7). As seen in section 5, sulfate is overall overpredicted. This is most of the time due to uncertainties in condensation and coagulation. For example, at Omiya and Kudan, Polair3D tends to overestimate the sulfate concentrations but CMAQ does not. Simulations without condensation or without coagulation give results that are similar to CMAQ, although both condensation and coagulation are taken into account in CMAQ. As discussed in section 5, the peaks of nitrate and ammonium are underpredicted on the 9^{th} at the stations above the meso-front: Omiya and Fukaya. When heterogeneous reactions are taken into account, the peaks are not underestimated any longer. However, they tend to be predicted earlier, stressing the difficulties of MM5 to accurately simulate the meso-front. Furthermore, the differences between Polair3D and CMAQ are often explained by the N_2O_5 heterogeneous reaction. If this heterogeneous reaction is taken into account, both Polair3D and CMAQ predict high nitrate and ammonium concentrations in the night and morning of the 9^{th} at all four stations and in the night and in the morning of the 10^{th} at Kudan, Omiya and Yokosuka. However, the high concentrations on the 10^{th} are not observed, suggesting the need to revise the rate of the N_2O_5 heterogeneous reaction. For example, *Evans and Jacob* [2005] suggest a rate that vary with the aerosol composition, temperature and relative humidity. The low nitrate and ammonium concentrations between the 9^{th} and the 10^{th} at Omiya are overpredicted by CMAQ because of the heterogeneous reactions. However, although the low nitrate concentrations are quite well predicted by Polair3D when heterogeneous reactions are ignored, the low ammonium concentrations are still overpredicted. Although nitrate concentrations are very small all through the episodes if condensation is not taken into account, ammonium concentrations are larger than the lowest observed concentrations. The unability of the model to reproduce the low ammonium concentrations may therefore be linked to uncertainties outside the aerosol module, most likely in the boundary conditions.

6.2. 31^{st} July and 1^{st} August 2001

In the summer episode, for sulfate, the impacts of the different processes are small compared to the impact of using CMAQ. The E_{NMAEF} for the simulation with CMAQ is equal to 0.55 against 0.08 for other simulations such as the one without condensation, the one using SIREAM and the one without deposition. The impact of condensation on sulfate is not as strong as it is in the winter episode. This suggests that sulfate mostly comes

from long-range transport. Whereas in the winter case, the averaged sulfate in the domain is larger than the averaged sulfate used for boundary conditions, the opposite holds in the summer case. The boundary condition for sulfate averaged over time, latitude and longitude is 16.6 μg m^{-3}, against a mean concentration of 13.5 μg m^{-3} in the domain of study. In fact, Mount Oyama of Miyake Island, which is located about 180km south of central Tokyo, was in eruption at that time (*Shinohara et al.* [2003]). Sulfate concentrations may be more sensitive to transport or diffusion processes, such as the parameterization used to model the vertical diffusion (*Mallet and Sportisse* [2006]) However, condensation influences to a great extent the nitrate and ammonium concentrations, with a E_{NMAEF} as large as 96.4 and 9.4 respectively. The impact of condensation on ammonium and nitrate is large compared to the impact of using CMAQ. Ammonium and nitrate are produced locally. Although condensation is largely a dominant process for the ammonium and nitrate concentrations, the influence of the hybrid simulation, where the thermodynamic equilibrium assumption is removed, is limited with a E_{NMAEF} of only 0.49 for nitrate and 0.18 for ammonium. The relative importance of the hybrid scheme versus condensation is higher in the winter episode than in the summer episode. Perhaps, this is because thermodynamic equilibrium is reached quickly under high temperatures (the mean temperature is 295K in the summer episode and 278K in the winter episode) and high pollutant concentrations (the averaged $PM_{2.5}$ concentration is 20.1μg m^{-3} in the summer episode and 13.3μg m^{-3} in the winter episode) (*Wexler and Seinfeld* [1990]). Nitrate concentrations, and ammonium concentrations to a lesser extent, are also strongly influenced by heterogeneous reactions with a E_{NMAEF} of 1.20 and 0.12 respectively. As for the winter case, the dominant heterogeneous reactions are the N_2O_5 and the NO_2 heterogeneous reactions. The E_{NMAEF} for the N_2O_5 heterogeneous reactions is as large as 0.95 for nitrate and 0.09 for ammonium. The impact of using SIREAM is not small although not preponderant: it is as large as the impact of deposition and condensation for sulfate, and it is as large as the impact of the hybrid scheme for ammonium and nitrate. Mode splitting, mode merging, nucleation and coagulation are negligible during this episode. Nucleation and coagulation are negligible in the summer case but not in the winter case. The mean temperature and relative humidity in the winter case are 278K and 49%, while they are 295K and 76% in the summer case. According to *Korhonen et al.* [2003], under these conditions of temperature and relative humidity, the nucleation rate is about 6 times higher in the winter case than in the summer case. The impact of coagulation is larger than the impact of nucleation, because coagulation does not only influence particles when they are freshly nucleated, but coagulation also influences these particles as they grow by condensation.

The impacts of the dominant processes during the episode are now investigated in more details, aiming at understanding the potential reasons for the discrepancies between measurements and simulated concentrations at the different stations (Figure 9). The sulfate concentrations are very little sensitive to the options used in the aerosol module in Polair3D, but large differences are observed between CMAQ and Polair3D. For example, at Kumagaya, Polair3D predicts lower sulfate concentrations than CMAQ in the night and morning of the 31^{st}, whereas it predicts higher sulfate concentrations later in the episode. Furthermore, the models exhibit stronger diurnal variations compared to observations. Because sul-

fate concentrations mostly come from long-range transport, and are little sensitive to options used in the aerosol module, the uncertainties in the sulfate concentrations are linked to uncertainties in the meteorology and boundary conditions. Polair3D and CMAQ use the same meteorological fields, except for the vertical diffusion, which is computed following *Troen and Mahrt* [1986] in Polair3D and following *CMAQ* [1999] (K-theory) in CMAQ. Uncertainty due to vertical diffusion is likely to be important as stressed by *Mallet and Sportisse* [2006]. Boundary conditions are provided on the vertical grid of CMAQ, which is used for the continental run, and they are projected onto the vertical grid of Polair3D. Uncertainties due to boundary conditions may not only be linked to this projection, but also to the projection of moments. Because the boundary conditions are obtained from CMAQ, they are given as the moments of order zero, two and three for particulate matter. However, a projection is required by Polair3D which uses the moments of order zero, three and six to represent particulate matter. Ammonium and nitrate are strongly influenced by condensation. Their concentrations are very low, and almost zero for nitrate, if condensation is not taken into account. As ammonia may condense onto aerosols to neutralize the sulfate, ammonium follows the diurnal evolution predicted for sulfate (the correlation between computed sulfate and ammonium is as high as 87%). Errors on ammonium concentrations are partly due to errors on sulfate concentrations. Another cause of errors may come from uncertainties in total ammonium. Ammonium concentrations are better predicted at Komae than at Kumagaya. As shown in Figure 10, the total ammonium concentration computed by Polair3D is higher at Komae than at Kumagaya, even though ammonium concentration in the aerosol phase is higher at Kumagaya. In the first part of the episode, at Kumagaya, the total ammonium computed is as low as the measured ammonium in the aerosol phase. Even though ammonium is systematically underestimated at Kumagaya, some discrepancies between modeled and observed ammonium can be explained by processes in the aerosol module at Komae. For example, whereas Polair3D overestimates ammonium concentrations in the afternoon of the 31^{st}, the ammonium concentrations are underestimated if the hybrid scheme is used. Nitrate is strongly underpredicted by Polair3D. However, the peaks of nitrate at night are better predicted when the N_2O_5 heterogeneous reaction is taken into account, although these peaks are sometimes overpredicted by CMAQ. As for total ammonium, total nitrate concentration is much higher at Komae than at Kumagaya (Figure 11). However, even though the total nitrate concentration is high at Komae, the high concentrations of nitrate in the aerosol phase in the afternoon of the 31^{st} at Komae are not reproduced even if the hybrid scheme is used. *Yu et al.* [2005] suggest that measurement uncertainties in sulfate and total ammonium, i.e. ammonium plus ammonia, can account for most of the discrepancies between the model predictions and observations in partitioning of aerosol nitrate.

7. Conclusion

In this article, two high-pollution episodes over Greater Tokyo are studied: one during the winter 1999 (9 and 10 December) and one during the summer 2001 (31 July and 1 August 2001). For each of these episodes, the chemistry transport model Polair3D is compared to measurements for inorganic components of $PM_{2.5}$.

For sulfate, error statistics are in agreement with

model performance criteria (*Yu et al.* [2006]). Inorganic components of $PM_{2.5}$ remain overall well modeled except for nitrate in the summer episode.

To understand to which extent the aerosol processes modeled in Polair3D influence the particle concentrations during the summer and the winter episodes, different simulations are made where only one process differs from the default or reference simulation. The following physical/chemical processes are considered: nucleation, coagulation, condensation/evaporation, whether condensation is modeled dynamically or using the thermodynamic equilibrium assumption, dry deposition, heterogeneous reactions. For numerical processes, the impact of mode merging/mode splitting and the impact of the size distribution (modal versus sectional) are evaluated. A comparison of the impact of each aerosol process described above to the impact of using the CTM CMAQ allows us to assess the importance of using different parameterizations and numerical schemes not only for aerosol processes but also for chemistry, transport and diffusion.

This study illustrates that the impact of aerosol processes on aerosol concentrations differs depending on local conditions and aerosol chemical components. For example, in the summer episode, for sulfate, the impact of long-range transport largely dominates. In the winter episode, sulfate is mostly impacted by condensation, coagulation, long-range transport, and deposition to a lesser extent. Whereas nucleation and coagulation are negligible in the summer episode, they are not in the winter episode. The impact of coagulation is larger in the winter episode than in the summer episode, because the number of small particles is higher in the winter episode as a consequence of nucleation. The impact of condensation/evaporation is dominant for ammonium, nitrate and chloride in both episodes. However, the impact of the thermodynamic equilibrium assumption is limited. The impact of heterogeneous reactions is large for nitrate and ammonium. The dominant heterogeneous reactions are the $NO_2 \rightarrow 0.5\ HONO + HNO_3$ and the $N_2O_5 \rightarrow 2\ HNO_3$ reactions. The impact of using a sectional representation of the size distribution is not negligible, and it is higher for ammonium and nitrate than for sulfate. The impact of mode merging/mode splitting is negligible in both episodes.

The comparison of the different runs also allows us to understand discrepancies between observed and simulated inorganic $PM_{2.5}$ at different stations. Heterogeneous reactions appear to be crucial in predicting the peaks of nitrate and ammonium in the winter episode. However, heterogeneous reactions sometimes lead to concentrations that are too high, suggesting the need for a more detailed parameterisation of the reaction rates.

Although the impact of mode merging and mode splitting is negligible on $PM_{2.5}$ concentrations, it may influence the size distribution of aerosols. Larger differences between the different runs may be observed by comparing the size distribution of aerosols or the concentrations of smaller particles such as PM_1. In particular, the impact of using a sectional rather than a modal model would be larger on the size distribution than on the mass of $PM_{2.5}$. The impact of nucleation and whether condensation is computed dynamically or using the thermodynamic assumption would be larger on PM_1 than on $PM_{2.5}$.

Acknowledgments.

This work was supported by the Canon Foundation in Europe, and by the program Primequal under the project PAM (Multiphase Air Pollution). We would like to thank the anonymous reviewers for their constructive comments on the manuscript.

Appendix A: Statistical Indicators

The following indicators are computed in order to evaluate error statistics for model-to-data comparisons. Let $(o_i)_i$ and $(c_i)_i$ be the observed and the modeled concentrations, where i is over n time series and locations, and $\bar{o} = \sum_{i=1}^{n} o_i$ and $\bar{c} = \sum_{i=1}^{n} c_i$ the averaged observed and modeled concentrations respectively

- Correlation

$$\frac{\sum_{i=1}^{n} (c_i - \bar{c})(o_i - \bar{o})}{\sqrt{\sum_{i=1}^{n} (c_i - \bar{c})^2} \sqrt{\sum_{i=1}^{n} (o_i - \bar{o})^2}} \quad \text{(A1)}$$

$$\text{with: } \bar{o} = \frac{1}{n} \sum_{i=1}^{n} o_i \text{ and } \bar{c} = \frac{1}{n} \sum_{i=1}^{n} c_i \quad \text{(A2)}$$

- Normalized mean bias factor (B_{NMBF})

$$\frac{\bar{c}}{\bar{o}} - 1 \text{ if } \bar{c} \geq \bar{o} \quad \text{(A3)}$$

$$1 - \frac{\bar{o}}{\bar{c}} \text{ if } \bar{c} < \bar{o} \quad \text{(A4)}$$

- Normalized mean absolute error factor (E_{NMAEF})

$$\frac{\sum_{i=1}^{n} |c_i - o_i|}{\bar{o}} \text{ if } \bar{c} \geq \bar{o} \quad \text{(A5)}$$

$$\frac{\sum_{i=1}^{n} |c_i - o_i|}{\bar{c}} \text{ if } \bar{c} < \bar{o} \quad \text{(A6)}$$

References

Binkowski, F., and S. Roselle (2003), Models-3 community multiscale air quality (CMAQ) model aerosol component 1. Model description, *J. of Geophys. Res.*, *108*(D6), 4183, doi:10.1029/2001JD001409.

Boutahar, J., S. Lacour, V. Mallet, D. Quelo, Y. Roustan, and B. Sportisse (2004), Development and validation of a fully modular platform for numerical modelling of air pollution: Polair3D, *International Journal of Environmental Pollution*, *22*(1-2).

CMAQ (1999), Science algorithms of the EPA models-3 community multiscale air quality (CMAQ) modeling system., *Tech. rep.*, U.S. Environmental Protection Agency, EPA/600/R-99/030.

Debry, E., K. Fahey, K. Sartelet, B. Sportisse, and M. Tombette (2007), A new SIze REsolved Aerosol Model: SIREAM, *Atmos. Chem. Phys. Discuss.*, *6*, 11,845–11,875.

Eder, B., and S. Yu (2006), A performance evaluation of the 2004 release of Models-3 CMAQ, *Atmos. Environ.*, *40*, 4811–4824.

Eder, B., D.W. Kang, R. Mathur, S. Yu, and K. Schere (2006), An operational evaluation of the Eta-CMAQ air quality forecast model, *Atmos. Environ.*, *40*, 4894–4905.

Evans, M.J, and D.J. Jacob (2005), Impact of new laboratory studies of N_2O_5 hydrolysis on global model budgets of tropospheric nitrogen oxides, ozone, and OH, *Geophys. Res. Let.*, *32*, L09813, doi:10.1029/2005GL022469.

Fujibe, F. (1985), Air pollution in the surface layer accompanying a local front at the onset of a land breeze, *J. Met. Soc. Japan*, *53*, 226–237.

Gery, M., G. Whitten, J. Killus, and M. Dodge (1989), A photochemical kinetics mechanism for urban and regional scale computer modeling, *J. of Geophys. Res.*, *94*(D10), 12,925–12,956.

A description of the fifth-generation Penn State/NCAR Mesoscale model (MM5), *NCAR Technical Note*, National Center for Atmospheric Research, Boulder, CO, NCAR/TN-398+STR.

Hayami, H. (2003), Inorganic ionic composition of aerosols collected in Kanto in summer, *Proc. the 44th Annual Meeting of Jap. Soc. for Atmos. Env.*, 162–163.

Hayami, H., and S. Fujita (2004), Concentrations and gas-aerosol partitioning of semi-volatile inorganic species measured with denuder/filter-pack sampling system in Tokyo., *J. of Jap. Soc. for Atmos. Env.*, *39*, 77–88.

Hayami, H., and S. Kobayashi (2004), Modeling of concentration of atmospheric secondary aerosol, *CRIEPI Technical Report*, Central Research Institute of Electric Power Industry, Japan, T03 037.

Jacob, D. (2000), Heterogeneous chemistry and tropospheric ozone, *Atmos. Environ.*, *34*, 2131–2159.

Kaneyasu, N., H. Yoshikado, T. Mizuno, K. Sakamoto, and M. Soufuku (1999), Chemical forms and sources of extremely high nitrate and chloride in winter aerosol pollution in the Kanto plain of Japan, *Atmos. Environ.*, *33*, 1745–1756.

Korhonen, H., K.E.J. Lehtinen, L. Pirjola, I. Napari, H. Vehkamki, M. Noppel, and M. Kulmala (2003), Simulation of atmospheric nucleation mode: a comparison of nucleation models and size distribution representations, *J. of Geophys. Res.*, *108*(D15), 4471, doi: 10.1029/2002JD003305.

Louis, J. (1979), A parametric model of vertical eddy fluxes in the atmosphere, *Boundary Layer Met.*, *17*, 187–202.

Mallet, V., and B. Sportisse (2006), Uncertainty in a chemistry-transport model due to physical parameterizations and numerical approximations: An ensemble approach applied to ozone modeling, *J. of Geophys. Res.*, *111*, D01302, doi:10.1029/2005JD006149.

Mebust, M., B. Eder, F. Binkowski, and S. Roselle (2003), Models-3 community multiscale air quality (CMAQ) model aerosol component 2. Model evaluation, *J. of Geophys. Res.*, *108*(D6), 4184, doi:10.1029/2001JD001410.

Mizuno, T., H. Kondo (1992), Generation of a local front and high levels of air pollution on the Kanto Plain in early winter, *Atmos. Environ.*, *26A*, 137–143.

Napari, I., M. Noppel, H. Vehkamaki, and M. Kulmala (2002), Parametrization of ternary nucleation rates for h_2so_4-nh_3-h_2o vapors., *J. of Geophys. Res.*, *107 (D19)*, doi: 10.1029/2002JD002132.

Nenes, A., S. Pandis, and C. Pilinis (1998), Isorropia : A new thermodynamic equilibrium model for multicomponent inorganic aerosols, *Aquatic geochemistry*, *4*, 123–152.

Ohara, T., I. Uno, and S. Wakamatsu (1990), Observational study of high concentration of NOx accompanied by the passage of land breeze front (in Japanese), *J. Japan Air Pollut. Ass.*, *25*, 66–76.

Ohara, T., S. Sugata, and T. Morikawa (2003), Urban pollution modeling in winter - Japan experience, *8^{th} International conference on Atmospheric Sciences and Application to Air Quality*, Tsukuba, Japan.

Roselle, S., K. Schere, and J. Pleim (1999), Photolysis rates for CMAQ, *Tech. rep.*, U.S. Environmental Protection Agency, EPA/600/R-99/030 chapter 14.

Sartelet, K., H. Hayami, B. Albriet, and B. Sportisse (2006), Development and preliminary validation of a modal aerosol model for tropospheric chemistry: MAM, *Aerosol Sci. and Tech.*, *40*(2), 118–127, doi:: 10.1080/02786820500485948.

Shinohara, H., K. Kazahaya, G. Saito, K. Fukui, and M. Odai (2003), Variation of CO_2/SO_2 ratio in volcanic plumes of miyakejima: Stable degassing deduced from heliborne measurements, *Geophys. Res. Lett.*, *30*, 1208, doi: 10.1029/2002GL016105.

Sportisse, B., K. Sartelet, E. Debry, K. Fahey, Y. Roustan, and M. Tombette (2006), The SIze REsolved Aerosol Model (SIREAM) and the Modal Aerosol Model (MAM). Technical documentation, *Tech. Rep. 8*, CEREA, 115 pages.

Stockwell, W., F. Kirchner, M. Kuhn, and S. Seefeld (1997), A new mechanism for Regional Atmospheric Chemistry Modeling, *J. of Geophys. Res.*, *95*(D10), 16,343–16,367.

Troen, I., and L. Mahrt (1986), A simple model of the atmospheric boundary layer: sensitivity to surface evaporation, *Boundary-Layer Meteorology*, *37*, 129–148.

Uno, I., T. Ohara, and S. Wakamatsu (1996), Analysis of wintertime NO_2 pollution in the Tokyo metropolitan area, *Atmos. Environ.*, *30*, 703–713.

Wakamatsu, S., I. Uno, T. Ohara, and K.L. Schere (1999), A study of the relationship between photochemical ozone and its precursor emissions of nitrogen oxides and hydrocarbons in Tokyo and surrounding areas, *Atmos. Environ.*, *33*, 3097–3108.

Wesely, M. (1989), Parameterization of surface resistance to gaseous-dry deposition in regional scale numerical models, *Atmos. Environ.*, *23*, 1293–1304.

Wexler, A., and J. Seinfeld (1990), The distribution of ammonium salts among a size and composition dispersed aerosol, *Atmos. Environ.*, *24A*(5), 1231–1246.

Whitby, E., F. Stratmann, and M. Wilck (2002), Merging and remapping modes in a modal aerosol dynamics models: a "dynamic mode manager, *J. of Aer. Sci.*, *33*, 623–645.

Yu, S., R. Dennis, S. Roselle, A. Nenes, J. Walker, B. Eder, K. Schere, J. Swall and W. Robarge (2005), An assessment if the ability of three-dimensional air quality models with current thermodynamic equilibrium models to predict aerosol NO_3^-, *J. of Geophys. Res.*, *110*, D07S13, doi: 10.1029/2004JD004718.

Yu, S., B. Eder, R. Dennis, S.-H. Chu and S.E. Schwartz (2006), New unbiased symmetic metrics for evaluation of air quality models, *Atmos. Sci. Let.*, *7*, 26–34.

Yu, S., R. Mathur, D.W. Kang, K. Schere, B. Eder and J. Pleirn (2006b), Performance and diagnostic evaluation of ozone predictions by the eta-community multiscale air quality forecast system during the 2002 New England Air Quality Study, *J. of the air management assoc.*, *56*(10), 1459-1471.

Zhang, L., S. Gong, J. Padro, and L. Barrie (2001), A size segregated particle dry deposition scheme for an atmospheric aerosol module, *Atmos.Environ.*, *35*, 549–560.

Zhang, L., P. Liu, A. Queen, C. Misenis, B. Pun, C. Seigneur, and S.-Y. Wu (2006), A comprehensive performance evaluation of MM5-CMAQ for the Summer 1999 Southern Oxidants Study episode – Part II: Gas and aerosol predictions, *Atmos.Environ.*, *40*, 4839–4855.

K. N. Sartelet, CEREA, Ecole Nationale des Ponts et Chaussées, 6-8 Avenue Blaise Pascal, 77455 Champs sur Marne, France. (sartelet@cerea.enpc.fr)

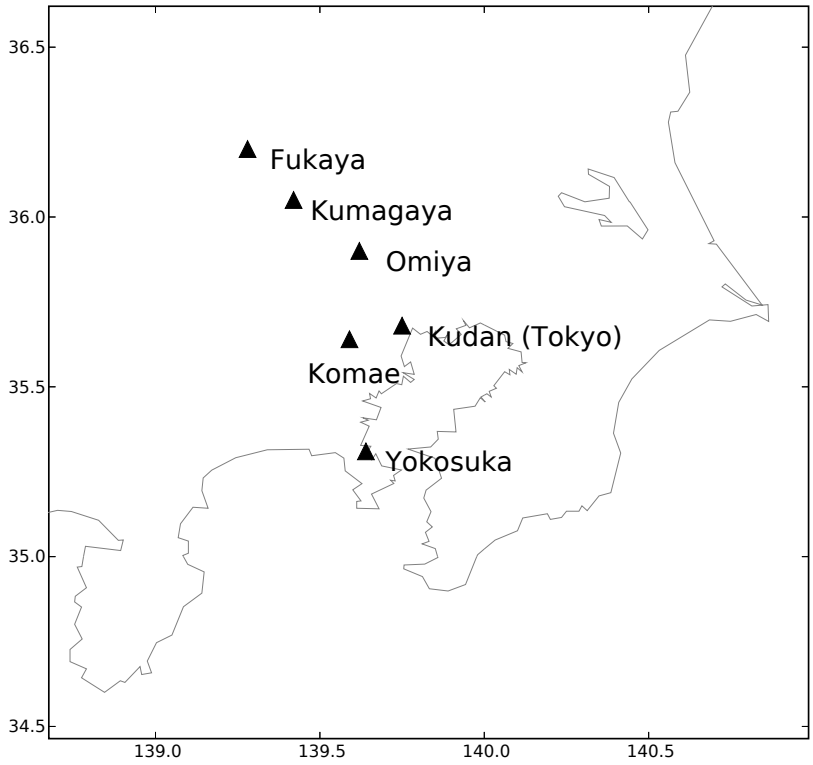

Figure 1. Location of stations at which the comparisons to data are made.

Table 1. Total amount (in kt) of emitted particulate matter and precursors over the domain (210km x 240km) for each episode.

	$PM_{2.5}$	PM_{10}	NO_x	SO_x	NH_3	HCl
Winter episode	0.44	0.23	3.72	1.75	0.54	0.16
Summer episode	0.40	0.23	2.82	1.24	1.81	0.15

Table 2. Parameters of the three modes used for emission.

	Aitken	Accumulation	Coarse
Mean Diameter (μm)	0.03	0.3	6
Standard Deviation	1.7	2	2.2

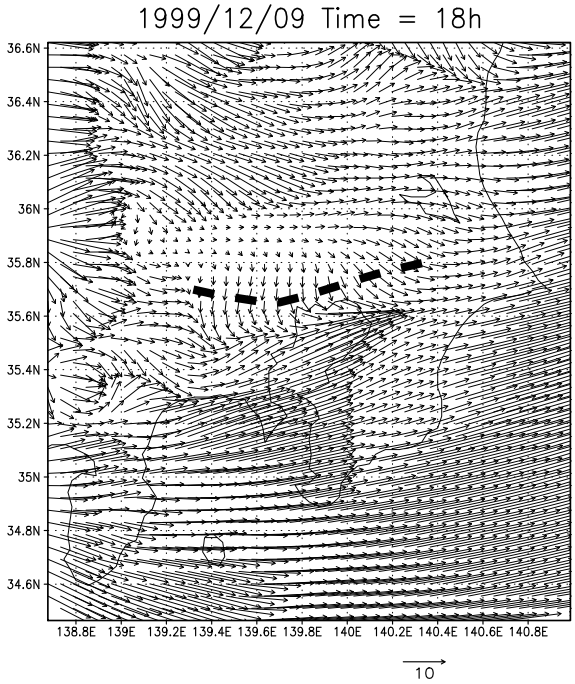

Figure 2. Wind vectors on 9 December at 6pm at 14.5m height (MM5 results). Black dashed line: observed meso-front.

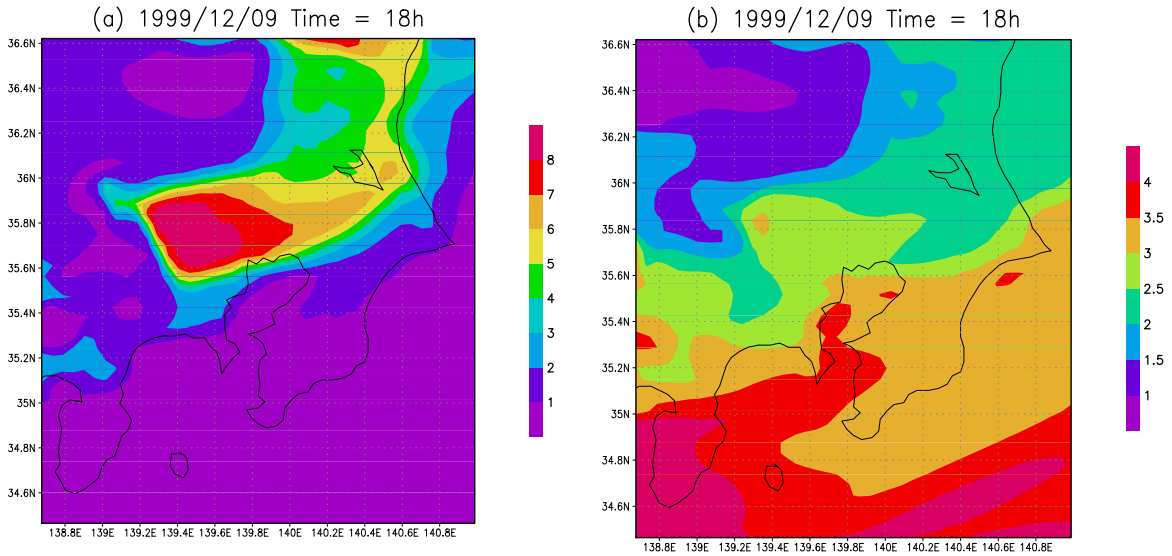

Figure 3. Modeled nitrate (panel a) and sulfate (panel b) concentrations on 9 December at 6pm.

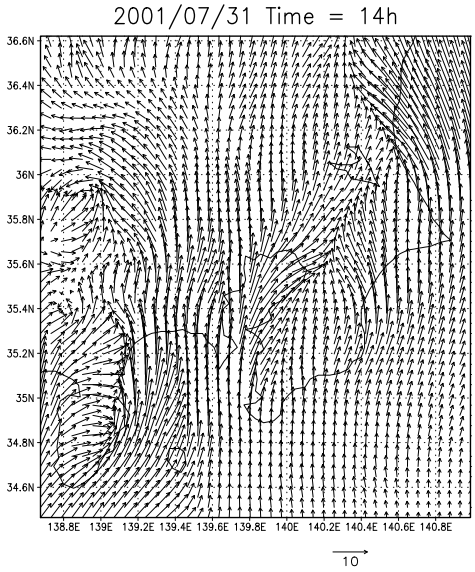

Figure 4. Wind vector at 2pm on 31 July.

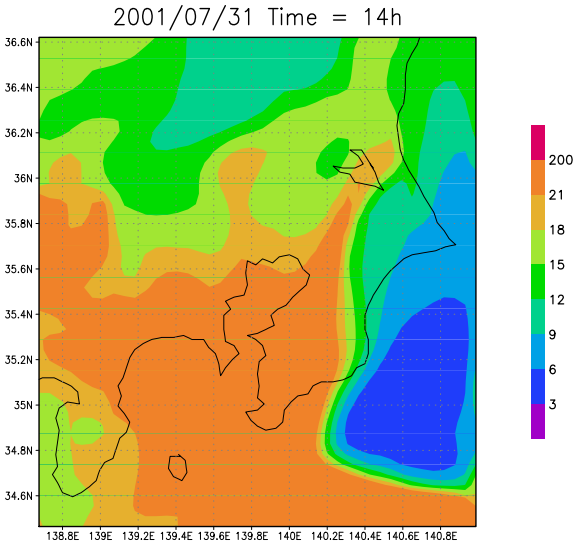

Figure 5. Modeled sulfate concentrations on 31 July at 2pm.

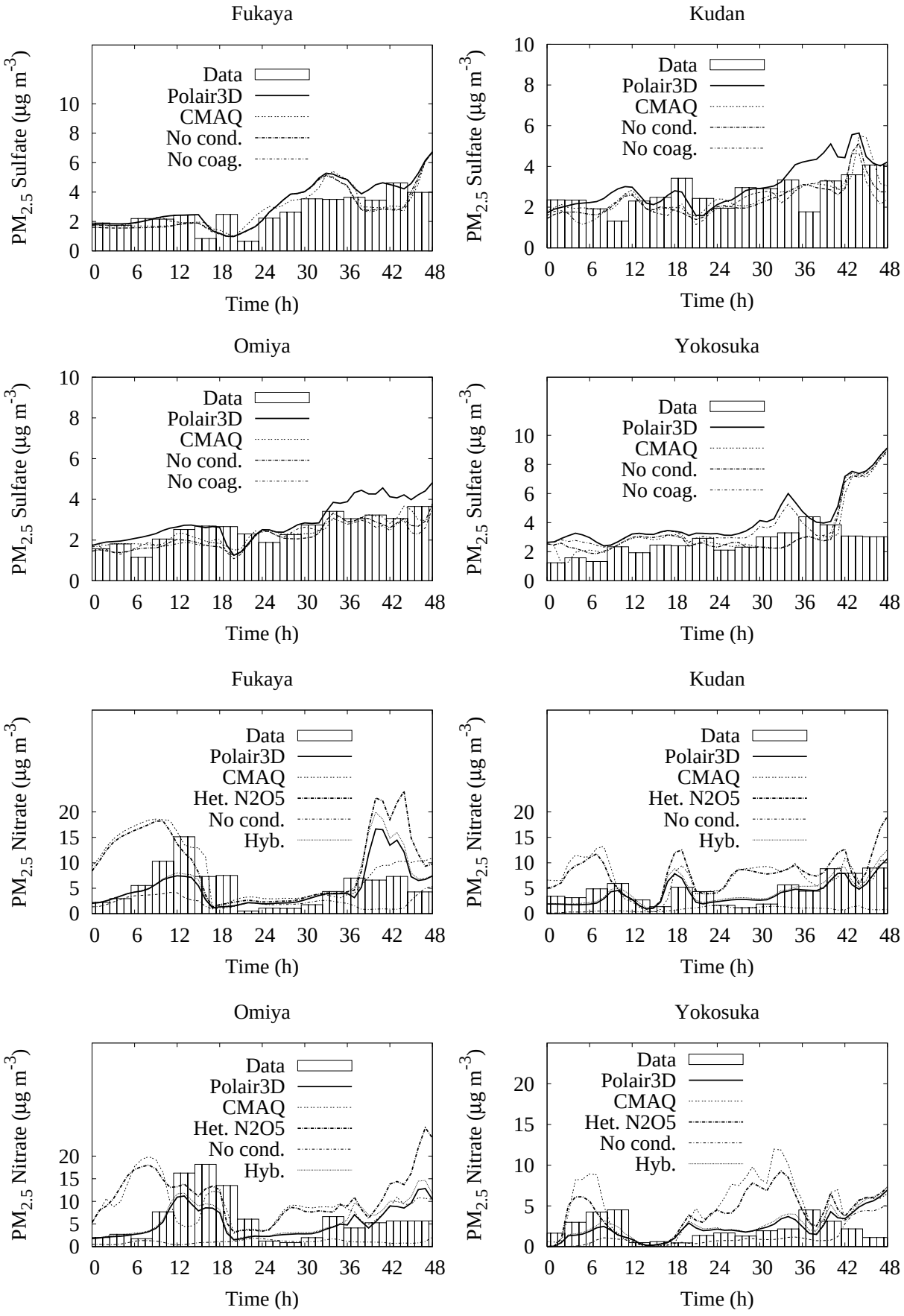

Figure 6. $PM_{2.5}$ concentration of sulfate and nitrate at Fukaya, Yokosuka, Kudan, Omiya for 9 and 10 December 1999.

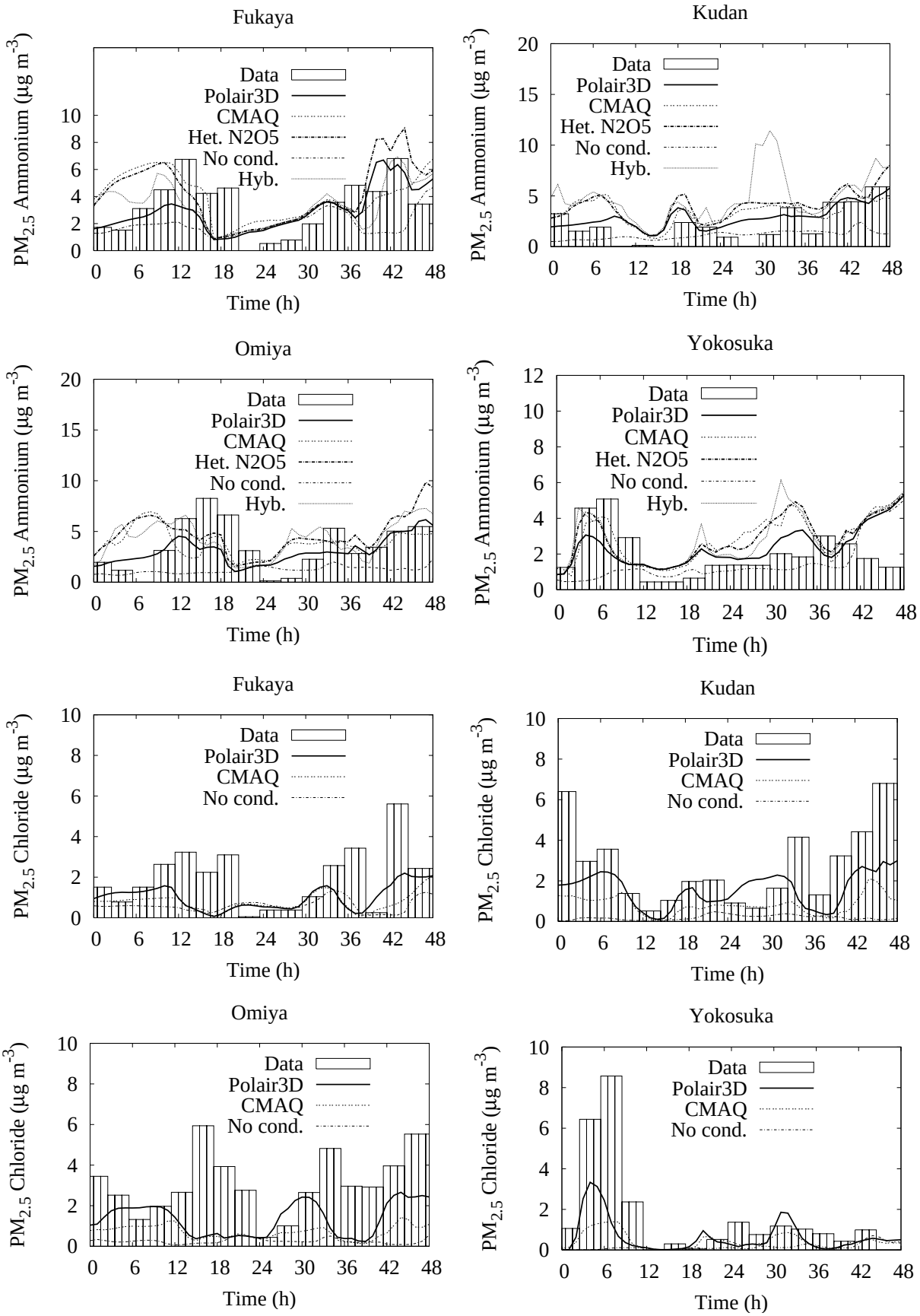

Figure 7. $PM_{2.5}$ concentration of ammonium and chloride at Fukaya, Yokosuka, Kudan, Omiya for 9 and 10 December 1999.

Table 3. Correlation (corr), B_{NMBF} and E_{NMAEF} obtained with Polair3D for 9 and 10 December 1999.

	corr	B_{NMBF}	E_{NMAEF}
Sulfate	66%	0.26	0.33
Ammonium	47%	0.05	0.56
Nitrate	45%	−0.10	0.58
Chloride	36%	−1.15	1.39
SO_2	44%	0.03	0.56

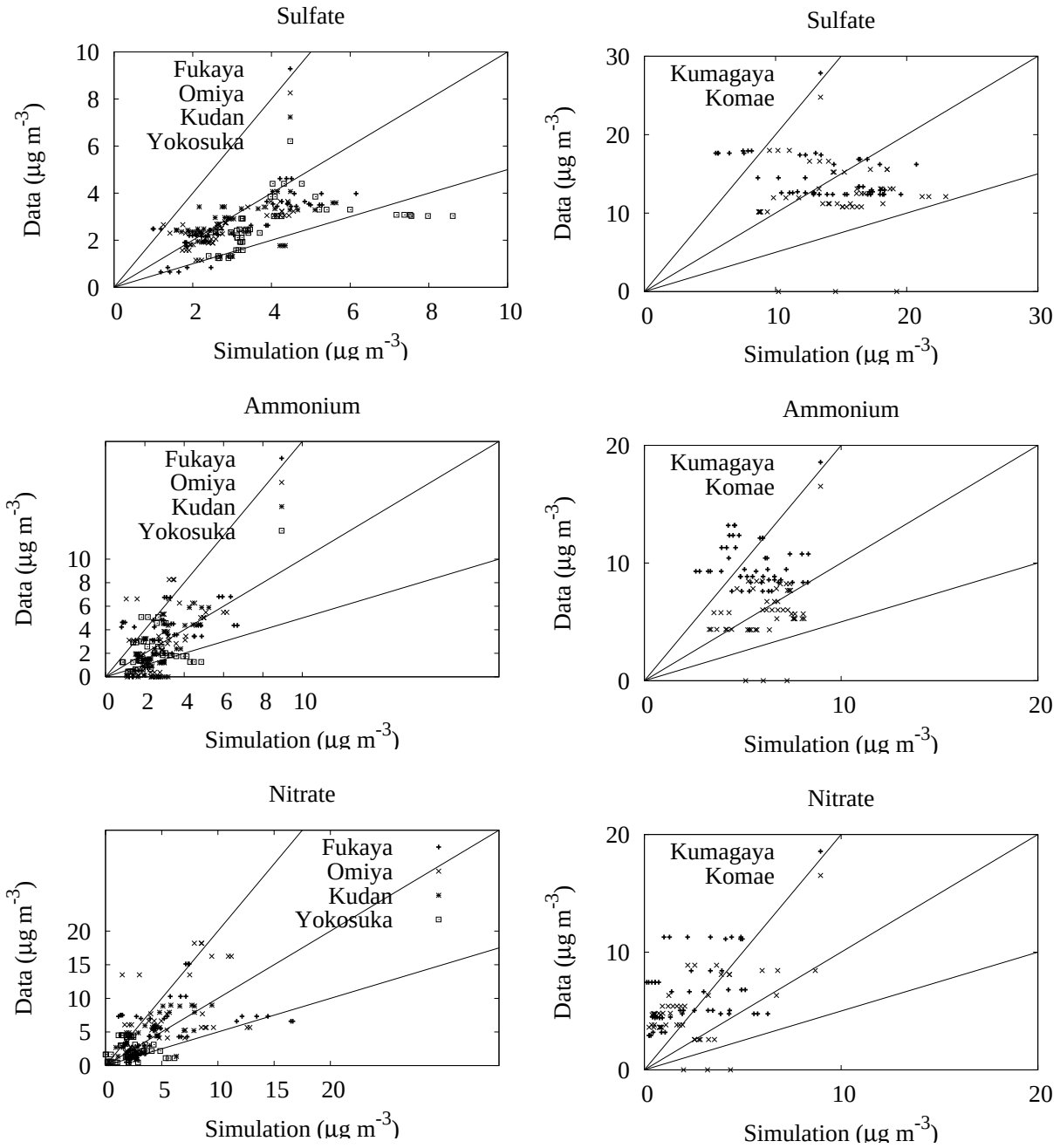

Figure 8. Scatter plots of observation (ordinate) versus simulation (abscissa) for sulfate, ammonium and nitrate for 9 and 10 December 1999 (left panels) and for 31 July and 1 August 2001 (right panels). 1:1, 1:2, and 2:1 reference lines are provided.

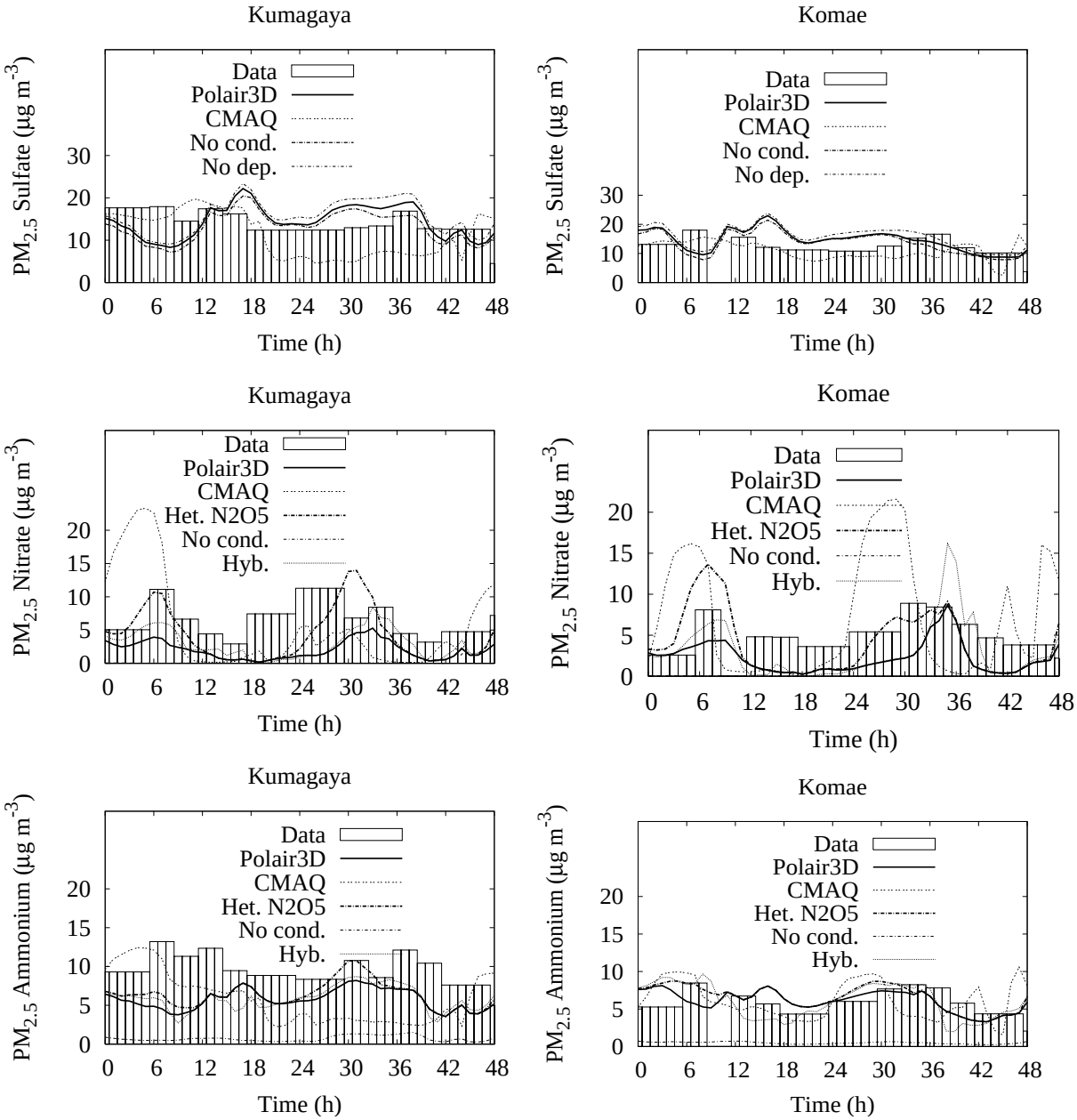

Figure 9. Comparisons of the $PM_{2.5}$ concentrations of sulfate, nitrate and ammonium at Kumagaya and Komae for 31 July and 1 August 2001 for different simulations.

Table 4. Correlation (corr), B_{NMBF} and E_{NMAEF} obtained with Polair3D and CMAQ for 31 July and 1 August 2001.

	corr	B_{NMBF}	E_{NMAEF}
Sulfate	−2%	0.11	0.32
Ammonium	12%	−0.30	0.49
Nitrate	34%	−1.73	1.85
SO_2	49%	0.04	0.45

Table 5. Comparison of Polair3D-MAM to different simulations for 9 and 10 December 1999: B_{NMBF} (B) and E_{NMAEF} (E).

	Sulfate		Ammonium		Nitrate		Chloride	
	B	E	B	E	B	E	B	E
No condensation	−0.27	0.27	−1.03	1.04	−2.44	2.44	−3.82	3.92
Hybrid	0.07	0.07	0.37	0.41	0.12	0.13	0.02	0.07
Het. React.	0.03	0.03	0.79	0.79	1.95	1.95	0.01	0.08
Only N_2O_5 het. react.	0.01	0.01	0.38	0.38	0.94	0.94	0.03	0.04
No NO_2 het. react.	0.01	0.01	0.38	0.38	0.93	0.93	0.03	0.04
No deposition	0.10	0.10	0.09	0.09	0.10	0.10	0.09	0.09
No nucleation	0.05	0.05	0.05	0.05	0.06	0.06	0.06	0.06
No coagulation	−0.21	0.21	−0.22	0.22	−0.25	0.25	−0.18	0.18
SIREAM	0.03	0.06	−0	0.05	−0.09	0.09	−0.08	0.08
Splitting	0.01	0.02	0.01	0.02	0.01	0.02	0.02	0.02
No merging - no splitting	−0.01	0.03	−0.01	0.03	−0.01	0.03	0	0.02
CMAQ	−0.21	0.24	0.26	0.38	0.85	1.00	−0.63	0.69

Table 6. Comparison of Polair3D-MAM to different simulations for 31 July and 1 August 2001: B_{NMBF} (B) and E_{NMAEF} (E).

	Sulfate		Ammonium		Nitrate	
	B	E	B	E	B	E
No condensation	−0.08	0.08	−9.40	9.40	−96.4	96.4
Hybrid	0.06	0.06	0	0.18	0.40	0.49
Het. React.	0	0	0.12	0.12	1.20	1.20
Only N_2O_5 het. react.	0	0	0.09	0.09	0.95	0.95
No NO_2 het. react.	0	0	0.09	0.09	0.92	0.93
No deposition	0.08	0.08	0.08	0.08	0.08	0.08
No nucleation	0.01	0.01	0.01	0.01	0.02	0.02
No coagulation	−0.01	0.01	−0.01	0.01	−0.02	0.02
SIREAM	−0.08	0.08	−0.11	0.11	−0.22	0.22
Splitting	0.02	0.02	0.02	0.02	0.02	0.02
No merging - no splitting	0.02	0.02	0.02	0.02	0.02	0.02
CMAQ	−0.32	0.55	−0.01	0.48	1.87	2.51

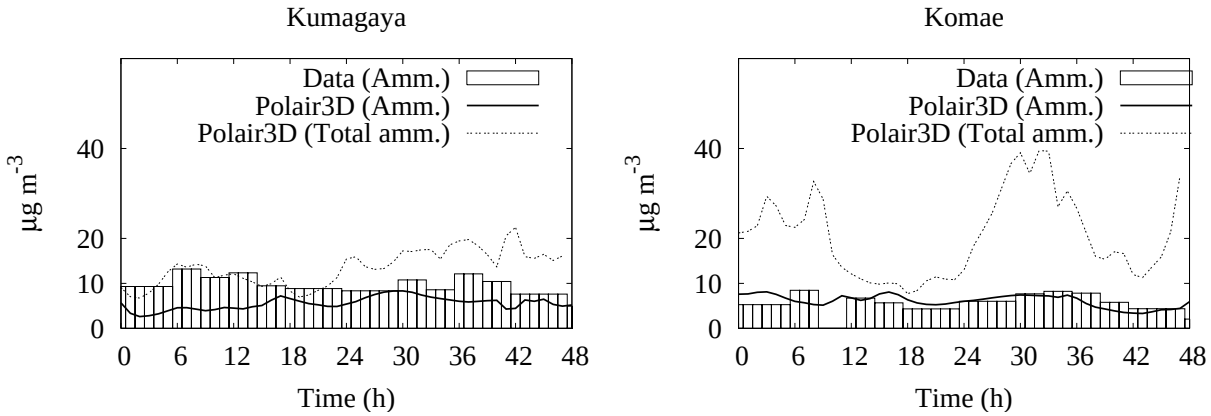

Figure 10. Concentrations of ammonium (modeled and observed) and total ammonium at Kumagaya and Komae for 31 July and 1 August 2001.

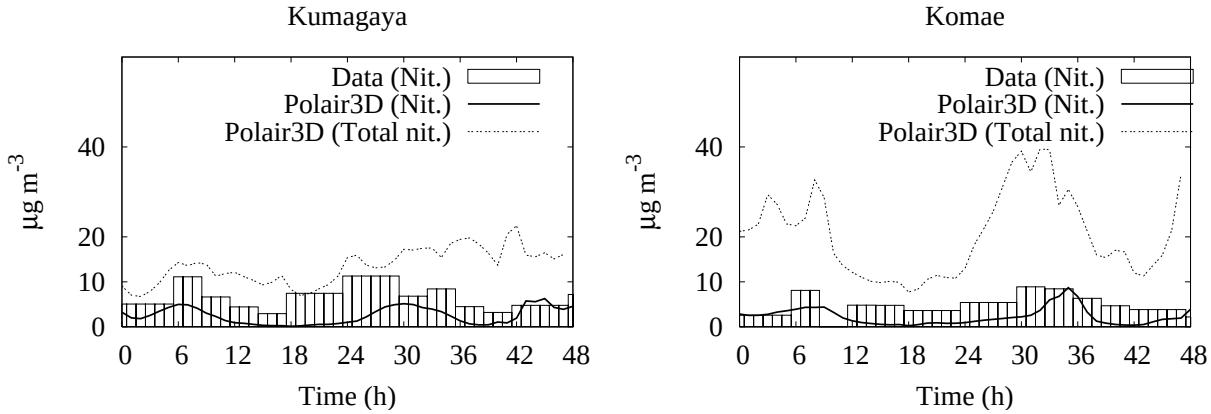

Figure 11. Concentrations of nitrate (modeled and observed) and total nitrate at Kumagaya and Komae for 31 July and 1 August 2001.